

Modelling of Surface Catalytic Reaction Systems using the Concept of Extents

Master thesis

by

Vibhuti Chhabra

In Partial Fulfilment of the Requirement for the Award of
Masters in Chemical Engineering & Biotechnology



ÉCOLE POLYTECHNIQUE
FÉDÉRALE DE LAUSANNE

Assistants: Dr. Julien Billeter, Sriniketh Srinivasan

Supervising Professor: Prof. Dominique Bonvin

Switzerland

04/09/2014

Acknowledgement

The completion of this Master thesis is a journey where I have been accompanied and supported by many people. I would like to take this opportunity to express my gratitude for all of them for accompanying me.

I am deeply grateful to Prof. Dominique Bonvin for providing me the facilities to conduct this research in his laboratory. His valuable advice during the presentation seminar and the constant support throughout the research is gratefully acknowledged.

I would like to thank my supervisor Dr. Julien Billeter for providing me with his support, perspective and mentorship during the course of the research. He was always ready to share his profound knowledge and provided constructive comments throughout to achieve the stated objectives. I would also like to thank him for correcting the clumsy sentences in the original manuscript.

I pay my sincere thanks to my supervisor Sriniketh Srinivasan for his valuable insights and inputs in the development of several concepts of the research. I am thankful that he always found time to listen to my questions, even the little ones, and gave his valuable advice.

I also thank Mateus Rodrigues Diogo Filipe for his time and interest in the project.

I warmly thank Mrs. Juillerat Karin for all her patience and support whenever needed. She has been a guardian to me throughout this journey.

I would also like to thank Mrs. Jenny Oswald for her valuable time and guidance regarding the administrative matters.

I am thankful to all my colleagues at the Laboratoire d'Automatique for such an enjoyable working atmosphere. I had opportunities to interact with interesting people and enjoyed the stimulating discussions on various spheres of life.

Last but not the least, I am especially grateful to my parents Mr. Daman Kumar Chhabra and Mrs. Anju Chhabra for their constant trust and support. They have been my backbone throughout this journey. I would take this opportunity to especially thank my mother who has also been my initial guide for this project.

Abstract

Gas-solid catalytic reaction systems depend on a combination of several dynamic effects, such as mass transfer, chemisorption and surface reactions taking place simultaneously. In this master thesis, the extension of the method of extent-based model identification is proposed for catalytic reaction systems which involves the transformation of the number of moles in the gas and solid phases into decoupled state variables called (vessel) extents. This transformation computes extents of inlet, outlet, mass transfer, initial conditions and invariants from the numbers of moles in the gas phase. From the numbers of moles in the solid phase, it also calculates extents of mass transfer, chemisorption (adsorption/desorption), surface reactions and invariants. Then, these extents can be used to perform incremental model identification, where each rate is identified individually based on its corresponding extent. This is illustrated through the simulated example of the ammonia synthesis (Haber-Bosch process) in a continuous stirred-tank reactor. For this system, correct rate models were identified and reliable rate parameters were estimated even in the presence of fast chemisorption and reaction processes. This however required a sufficiently large amount of measurements at the start of the synthesis. Future work should focus on the extension of this method to more complex catalytic schemes involving more intermediate species.

Keywords Heterogeneous catalysis, extents-based model identification, kinetic modelling, ammonia synthesis

Contents

| | |
|--|------------|
| Abstract | iii |
| 1 Introduction | 1 |
| 1.1 External Mass Transfer | 2 |
| 1.2 Internal Mass Transfer | 2 |
| 1.3 Combined Mass Transfer | 3 |
| 1.4 Chemisorption and Reaction on the Catalyst Surface | 3 |
| 1.5 Identification of the Rate Determining Step | 4 |
| 2 Mole Balance Equations | 6 |
| 2.1 Gas Phase | 7 |
| 2.2 Solid Phase | 7 |
| 3 Kinetic Identification using Extents | 9 |
| 3.1 Transformation to Extents | 9 |
| 3.1.1 Gas Phase | 10 |
| 3.1.2 Solid Phase | 12 |
| 3.2 Kinetic Identification | 15 |
| 4 Case Study | 16 |
| 4.1 Reaction System | 16 |
| 4.2 Simulated Measurements | 17 |
| 4.3 Computation of Extents | 20 |
| 4.4 Identification of Rate Expressions | 21 |
| 5 Conclusion | 24 |

List of Figures

| | | |
|-----|---|----|
| 1.1 | <i>Mechanism of a typical catalytic reaction taking place in seven steps: (1) External diffusion (mass transfer), (2) Internal diffusion (mass transfer), (3) Adsorption on the active sites, (4) Surface reaction forming the products, (5) Desorption of the products, (6) Internal diffusion (mass transfer) and (7) External diffusion (mass transfer). Taken from Fogler [3].</i> | 1 |
| 1.2 | <i>Within small boundaries, mass transfer occurs by (a) bulk (free space) diffusion or (b) Knudsen diffusion, that is, when the particles free motion is restricted by the wall dimensions. Taken from [6].</i> | 2 |
| 1.3 | <i>Electric analogue circuit depicting the flux of the diffusion from a gas to a porous medium. Adapted from [7].</i> | 3 |
| 2.1 | <i>Schematic description of a Gas-Solid catalytic reaction system with two bulk phases connected by mass-transfer phenomena.</i> | 6 |
| 3.1 | <i>Decomposition of the S_g-dimensional space of the numbers of moles in the gas phase into a p_g-dimensional inlet subspace, a p_m-dimensional mass-transfer subspace, a one-dimensional subspace describing the contribution of the initial conditions and a q_g-dimensional invariant subspace.</i> | 10 |
| 3.2 | <i>Decomposition of the S_s-dimensional space of the numbers of moles in the solid phase into a p_m-dimensional mass transfer subspace, a p_a-dimensional chemisorption subspace, a R-dimensional reaction subspace and a q_s-dimensional invariant subspace.</i> | 13 |
| 4.1 | <i>(Simulated) measurements of the number of moles in the gas phase (a) and in the solid phase (b), coverage of the reaction intermediates (c), reaction yield (d), turnover frequency (TOF) (e) and total pressure in the reactor (f) as a function of time.</i> | 19 |
| 4.2 | <i>Extents of inlet ($\mathbf{x}_{in,g}$, diagram A), of initial conditions ($\mathbf{x}_{ic,g}$, diagram B) and of mass transfer ($\mathbf{x}_{m,g}$, diagram C) in the gas phase and extents of mass transfer ($\mathbf{x}_{m,s}$, diagram D), of chemisorption (\mathbf{x}_a, diagram E) and of reaction (\mathbf{x}_r, diagram F) in the solid phase as a function of time.</i> | 21 |
| 4.3 | <i>Extents of chemisorption (A: $x_{a,1}$, B: $x_{a,2}$ and C: $x_{a,3}$) and of reaction (D: $x_{r,1}$, E: $x_{r,2}$, F: $x_{r,3}$ and G: $x_{r,4}$) over time obtained by transformation of the measured numbers of moles (in blue) and integration of the correctly identified rate expression (in red).</i> | 22 |

List of Tables

| | | |
|-----|---|----|
| 2.1 | Number of species and dynamic effects in each phase of a Gas-Solid reaction system. | 6 |
| 4.1 | Reactor characteristics (taken from [22]) | 16 |
| 4.2 | Catalyst characteristics (taken from [3, 5, 6, 7, 24]) | 17 |
| 4.3 | Number of species and number of dynamic effects involved in the synthesis of ammonia . . . | 18 |
| 4.4 | Identified rate expressions and estimated rate constants in $(\text{mol}/\text{m}^2)^{-1}\text{s}^{-1}$ (with 99% confidence intervals, C.I.) for all reaction steps of the synthesis of ammonia. | 23 |
| 4.5 | Identified rate expressions and estimated rate coefficients (with 99% confidence intervals, C.I.) for all chemisorption steps involved in the synthesis of ammonia. | 23 |

Chapter 1

Introduction

Catalysts are substances that speed up reactions by providing an alternative pathway for the breaking and formation of bonds. Key to this alternative pathway is a lower activation energy than that required for an uncatalysed reaction. Industrially, catalysts are widely used to produce highly selective products. Catalysts are used in various industrial processes like ammonia synthesis, production of syngas and cracking of gas oil.

The research in the field of catalysis focuses on improving the efficiency of catalytic reactions. As these systems are not only controlled by surface reactions but also influenced by mass transfers and chemisorption, it is important to study the effect of each phenomenon individually to improve the catalytic activity.

This chapter introduces the phenomena involved in Gas-Solid heterogeneous catalytic systems, where the catalyst is the solid phase and the species that react on the surface of the catalyst are coming from the gas phase. Heterogeneous catalytic systems can be defined as reaction systems where the catalyst is in a different phase than the reactants or products. These types of reaction systems are often favoured in industry as the two phases can be easily separated during downstream processing.

The reaction mechanism of these catalytic systems have seven elementary steps depicted in Figure 1.1: (1) External diffusion (mass transfer), (2) Internal diffusion (mass transfer), (3) Adsorption on the active sites, (4) Surface reaction forming the products, (5) Desorption of the products, (6) Internal diffusion (mass transfer) and (7) External diffusion (mass transfer) [3]. Each physical phenomenon is described in details in the following sub-sections.

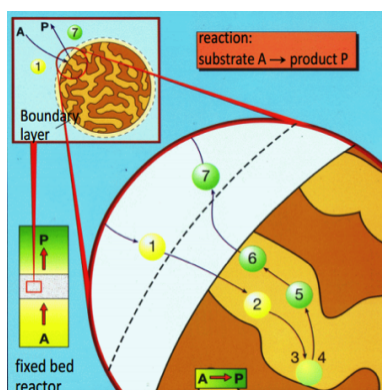


Figure 1.1: Mechanism of a typical catalytic reaction taking place in seven steps: (1) External diffusion (mass transfer), (2) Internal diffusion (mass transfer), (3) Adsorption on the active sites, (4) Surface reaction forming the products, (5) Desorption of the products, (6) Internal diffusion (mass transfer) and (7) External diffusion (mass transfer). Taken from Fogler [3].

1.1 External Mass Transfer

The transfer of the gas species from the gas bulk to the gas-solid interface is called external mass transfer. In general the mass transfer phenomena are governed by interfacial concentrations that are difficult to observe experimentally. Thus, the problem is simplified by assuming a steady-state mass transfer, that is, no accumulation in the boundary layer.

The external mass transfer can be modelled by various approaches such as the stagnant film model, the Higbie penetration theory, the surface renewal theory, the film penetration model, and their modifications [4, 5].

A simple way to model the mass-transfer phenomena is the stagnant film model, which states that all the resistance to mass transfer comes from a thin stagnant film at the interface of the two phases in contact [4]. The rate of steady-state mass transfer can be calculated by the Fick's first law, which computes the molar flux (in units $\frac{\text{moles}}{\text{area} \cdot \text{time}}$) for each species that transfers from the gas to the gas-solid interface [4]. The rate of mass transfer ξ_i^{ext} (in units $\frac{\text{moles}}{\text{time}}$) for the i th species involved in a laminar flow at steady-state is calculated as

$$\xi_i^{ext}(t) = -A^{ext} \frac{D_i^{ext}}{z^{ext}} \left(\frac{\Delta p_i^{ext}(t)}{RT} \right) = -A k_{m,i}^{ext} \Delta c_i^{ext}(t) \quad (1.1)$$

where D_i^{ext} is the external diffusion coefficient of the i th species transferring through the film of thickness z^{ext} (with $k_{m,i}^{ext} = \frac{D_i^{ext}}{z^{ext}}$), A^{ext} is the external interfacial surface area of the catalyst and $\Delta c_i^{ext} = \frac{\Delta p_i^{ext}}{RT}$ is the difference of concentration for the i th species between the gas and the gas-solid interface.

1.2 Internal Mass Transfer

The Internal mass transfer is the diffusion of the fluid mixture inside the porous matrix of the catalyst. Within a pore, mass transfer phenomena are governed by various diffusion mechanisms, namely, (a) bulk (free space) diffusion and (b) Knudsen diffusion, as shown in Figure 1.2 [6]. These simultaneous diffusion processes make the internal mass transfer slower than the external mass transfer.

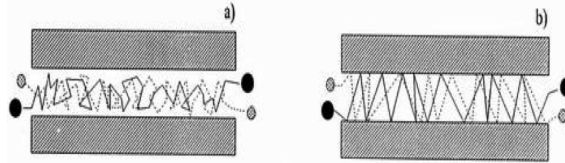


Figure 1.2: Within small boundaries, mass transfer occurs by (a) bulk (free space) diffusion or (b) Knudsen diffusion, that is, when the particles free motion is restricted by the wall dimensions. Taken from [6].

Using Fick's first law, the molar flux (in units $\frac{\text{moles}}{\text{area} \cdot \text{time}}$) for each species that transfers from the gas-solid interface to the inside of the pores can be computed. The rate of steady-state mass transfer ξ_i^{int} (in units $\frac{\text{moles}}{\text{time}}$) for the i th species is calculated as

$$\xi_i^{int}(t) = -A^{int} \frac{D_i^{int}}{z^{int}} \left(\frac{\Delta p_i^{int}(t)}{RT} \right) = -A k_{m,i}^{int} \Delta c_i^{int}(t) \quad (1.2)$$

where D_i^{int} is the internal diffusion coefficient of the i th species transferring through pores of length z^{int} (with $k_{m,i}^{int} = \frac{D_i^{int}}{z^{int}}$), A^{int} is the internal interfacial surface area of the catalyst and $\Delta c_i^{int} = \frac{\Delta p_i^{int}}{RT}$ is the difference of concentration for the i th species between the gas-solid interface and the inside of the pores. Note that the diffusion coefficients for the internal mass transfer are generally much lower in magnitude than the ones for the external mass transfer ($D_i^{int} \ll D_i^{ext}$).

1.3 Combined Mass Transfer

As depicted in Figure 1.3, the two diffusion (mass transfer) processes occur in series and hence both phenomena can be combined as [6]

$$\xi_{m,i}(t) = -A \frac{D_i}{z} \left(\frac{\Delta p_i(t)}{RT} \right) = -A k_{m,i} \Delta c_i(t)$$

where

$$\frac{1}{A D_i} = \frac{1}{A^{ext} D_i^{ext}} + \frac{1}{A^{int} D_i^{int}}$$

$$\frac{1}{z k_{m,i}} = \frac{1}{z^{ext} k_{m,i}^{ext}} + \frac{1}{z^{int} k_{m,i}^{int}} \quad (1.3)$$

$$\Delta p_i(t) = \Delta p_i^{ext}(t) + \Delta p_i^{int}(t)$$

and $z = z^{ext} + z^{int}$

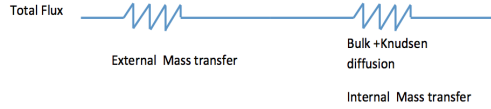


Figure 1.3: *Electric analogue circuit depicting the flux of the diffusion from a gas to a porous medium. Adapted from [7].*

As there is no structural difference between a species diffusing from a gas to a gas-solid interface or from a gas-solid interface to the inside of the pores of the solid, except the value of the overall diffusion coefficient D_i and how the difference Δp_i is computed, the term 'solid surface' will be used here interchangeably to indicate gas-solid interface or (if applicable) the inside of the pores of the solid surface.

For p_m species transferring from a gas to the solid surface (or the inside of the pores), the p_m overall rates of mass transfer can be gathered in a vector ξ_m expressed in $\frac{mole}{time}$. By convention, mass transfer from the gas to the solid surface is positive whereas mass transfer from the solid surface to the gas is negative.

1.4 Chemisorption and Reaction on the Catalyst Surface

The species that reach by mass transfer the solid surface are chemically adsorbed on the catalyst surface. The adsorbed species then react with each other and form products which are finally desorbed. The adsorption and desorption phenomena are usually referred together as chemisorption.

A wide variety of isotherm models at equilibrium (Langmuir, Freundlich, Brunauer-Emmett-Teller (BET), Redlich Peterson, Dubinin Radushkevich, Temkin, Toth, Koble Corrigan, Sips, Khan, Hill, Flory-Huggins and Radke Prausnitz isotherms) have been formulated to represent this chemisorption process [8]. A simple model that describes the bimolecular catalytic reaction is the Langmuir-Hinshelwood (L-H) model.

L-H isotherm states that molecules are adsorbed on particular sites of the catalyst which are called the active sites and denoted $*$. Only one molecule is assumed to be adsorbed per active site. L-H isotherm decomposes the catalytic reactions in three steps.

For a bimolecular catalytic reaction of the form $A + B \rightarrow C$, the three steps are the following [8]:

1. the reactants A and B are instantaneously adsorbed on two vacant active sites $*$ (competitive adsorption) without dissociation,

2. the slow step is the reaction between the two adsorbed reactants, denoted A^* and B^* ,
3. the product C is weakly adsorbed, that is, C^* is instantaneously desorbed.

The chemisorption and reaction processes can be combined as a set of 'physical' and 'chemical' reactions at the solid surface, defined with an A (for adsorption) or a R (for reaction) followed by a number, respectively.



In the above set of reactions, A , B and C represent the species just above the solid surface in the gas phase, A^* , B^* and C^* their corresponding adsorbed species, and $*$ represents the vacant active sites on the catalyst surface.

As all the reactions occur at the surface of the catalyst, the rate is defined in units $\frac{\text{moles}}{\text{area} \cdot \text{time}}$. The concentration of species present on the catalyst surface, denoted \mathcal{C} , are defined in units $\frac{\text{moles}}{\text{area}}$ [9]. The units of the rate constant for a n^{th} order reaction is $\text{moles}^{(1-n)} \cdot \text{area}^{(n-1)} \cdot \text{time}^{-1}$.

For p_a chemisorption reactions, p_a species are transferred to the solid surface. The overall rates of chemisorption are gathered in a vector ξ_a calculated by multiplying the rates of chemisorption and the surface area of the catalyst A . By convention all chemisorption reactions are assumed to be adsorption processes, thus the positive sign (+) implies that a species is adsorbed and a negative sign (-) implies that the species is desorbed from the solid surface. For the R reactions, the overall rates of reaction are gathered in a vector \mathbf{r} calculated by multiplying the rates of reaction and the surface area of the catalyst A .

Note 1: The total concentration of active sites (occupied Ω or free) on a catalyst surface remains constant at \mathcal{C}_{tot} . Thus the concentrations of all the adsorbed species are linearly dependent on each other as follows:

$$\mathcal{C}_* + \sum \mathcal{C}_\Omega = \mathcal{C}_{tot}, \quad \text{where } \Omega \in \{A^*, B^*, C^*\} \quad (1.8)$$

with \mathcal{C}_* the concentration of the vacant active sites.

Note 2: The adsorbed species can be expressed in terms of surface coverage θ_Ω , which is the ratio of concentrations and the total number of active sites, that is, $\theta_\Omega = \frac{\mathcal{C}_\Omega}{\mathcal{C}_{tot}}$. Similarly, the coverage of the vacant sites is defined as $\theta_* = \frac{\mathcal{C}_*}{\mathcal{C}_{tot}}$. The sum of the coverages of all species are also linearly dependent on each other as

$$\theta_* + \sum \theta_\Omega = \frac{\mathcal{C}_*}{\mathcal{C}_{tot}} + \sum \frac{\mathcal{C}_\Omega}{\mathcal{C}_{tot}} = 1 \quad (1.9)$$

1.5 Identification of the Rate Determining Step

As the rate coefficients of all involved phenomena are very different, the major challenge is to determine the rate limiting step of the catalytic reaction system. This section discusses the difficulties of estimating the true rate of reaction if the system is limited by either of the two mass transfers.

Case 1 External mass transfer is limiting

If the external diffusion coefficients D_i^{ext} are very small, the rate of reaction is limited by the external diffusion. Obviously, this implies that the surface reactions are very fast compared to the external mass transfer diffusion. In this case, the observed reaction kinetics will appear slower than it is actually, which means that the catalyst is inefficient [3].

Case 2 Internal mass transfer is limiting

If the internal diffusion coefficients D_i^{int} are very small, the rate of reaction is limited by the internal diffusion. This implies that the surface reactions are very fast compared to the internal mass transfer, which means that the observed reaction kinetics will appear slower than it is actually [3].

Case 3 Reactions are limiting

In this case, the true kinetics is observed.

For these reasons, it is important to operate a reactor in conditions that ensure that the system is not limited by any mass transfer by diffusion.

This chapter has introduced the mechanism of a heterogeneous catalytic systems that is the used in the next chapter to formulate the mole balance equations for a Gas-Solid catalytic reaction system. The third chapter describes the transformation of the number of moles in both phases to their corresponding extents. In the fourth chapter, the case study of the ammonia synthesis (Haber-Bosch process) is simulated and analysed to illustrate the implementation of the concepts developed in this thesis. The last chapter concludes this thesis.

Chapter 2

Mole Balance Equations

A schematic description of a Gas-Solid catalytic reaction system is shown in Figure 2.1, where the solid phase represents the catalyst surface on which reactions take place.

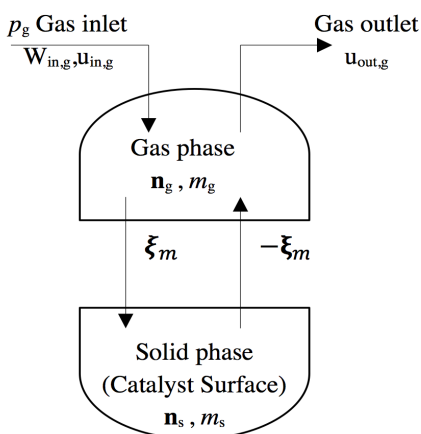


Figure 2.1: Schematic description of a Gas-Solid catalytic reaction system with two bulk phases connected by mass-transfer phenomena.

Such a Gas-Solid reaction system can be described by the number of species and dynamic effects in each of its phase, as seen in Table 2.1.

Table 2.1: Number of species and dynamic effects in each phase of a Gas-Solid reaction system.

| Phase | Species | Inlet streams | Outlet stream | Mass transfers | Chemisorptions | Reactions |
|-------------|---------|---------------|---------------|----------------|----------------|-----------|
| Gas phase | S_g | p_g | 1 | p_m | 0 | 0 |
| Solid phase | S_s | 0 | 0 | p_m | p_a | R |

In Table 2.1, S_g is the number of species in the gas phase that transfer to and from the solid catalyst surface through p_m mass transfers. The rates of mass-transfer are gathered in a vector ξ_m , with the sign convention defined in Section 1.3. The transferred species are chemisorbed (i.e. adsorbed or desorbed) on the catalyst surface via p_a chemisorption processes. The rates of chemisorption are gathered in a vector ξ_a , with the sign convention introduced in Section 1.4. The chemisorbed species undergo R surface reactions whose rates are collected in a vector \mathbf{r} .

S_s represents the total number of species in the solid phase, namely, the free reactants and product just above the catalyst surface, the reactants, products and possible intermediates that are adsorbed on the surface of the catalyst and the vacant active sites of the catalyst. Note that in absence of reactions in the gas phase, $S_s > S_g$.

Let us consider in more details the assumptions made in Table 2.1 and other useful assumptions that can be made to simplify the modelling of such a system:

1. The solid surface and the gas phase are homogeneous (well mixed),
2. The gas phase has a constant density,
3. The solid phase has a constant area,
4. The reactions take place in the solid phase only, and
5. The mass transfers are at steady state (no accumulation in the boundary layer).

Under these assumptions, the mole balances for the gas and solid phases can be described as two sets of Ordinary Differential Equations (ODE), which are introduced next.

2.1 Gas Phase

The mole balance for the gas phase reads:

$$\dot{\mathbf{n}}_g(t) = \mathbf{W}_{in,g} \mathbf{u}_{in,g}(t) - \mathbf{E}_{m,g} \boldsymbol{\xi}_m(t) - \frac{u_{out,g}(t)}{m_g(t)} \mathbf{n}_g(t), \quad \mathbf{n}_g(0) = \mathbf{n}_{0,g} \quad (2.1)$$

Where \mathbf{n}_g is a S_g dimensional vector containing the number of moles in the gas phase, $\mathbf{W}_{in,g} = \mathbf{M}_{w,g}^{-1} \check{\mathbf{W}}_{in,g}$ is the $S_g \times p_g$ matrix for the composition of the inlet streams, with $\mathbf{M}_{w,g}$ the S_g -dimensional diagonal matrix of molecular weights and $\check{\mathbf{W}}_{in,g} = [\check{\mathbf{w}}_{in,g}^1, \dots, \check{\mathbf{w}}_{in,g}^{p_g}]$ a $S_g \times p_g$ matrix where $\check{\mathbf{w}}_{in,g}^i$ is a S_g dimensional vector containing the weight fractions of the S_g species in the i th inlet stream, $\mathbf{u}_{in,g}$ is a p_g dimensional vector containing the mass flowrates of the p_g streams into the reactor, $\mathbf{E}_{m,g} = [\mathbf{e}_{m,g}^1, \dots, \mathbf{e}_{m,g}^{p_m}]$ is $S_g \times p_m$ matrix with $\mathbf{e}_{m,g}^j$ being a S_g dimensional vector with the element corresponding to the j th mass transfer transferring species equal to unity and the other elements equal to zero, and $u_{out,g}$ is the mass flowrate of the outlet stream from the reactor.

The mass in the gas phase $m_g(t)$ can be calculated from the number of moles $\mathbf{n}_g(t)$ as

$$m_g(t) = \mathbf{1}_{S_g}^T \mathbf{M}_{w,g} \mathbf{n}_g(t), \quad m_g(0) = m_{0,g} \quad (2.2)$$

with $\mathbf{1}_{S_g}^T$ a S_g -dimensional vector of ones.

2.2 Solid Phase

The mole balance of the solid phase can be written as:

$$\dot{\mathbf{n}}_s(t) = \mathbf{E}_{m,s} \boldsymbol{\xi}_m(t) + \mathbf{N}_a^T \boldsymbol{\xi}_a(t) + \mathbf{N}_r^T \mathbf{r}(t), \quad \mathbf{n}_s(0) = \mathbf{n}_{0,s} \quad (2.3)$$

where \mathbf{N}_a^T is the $S_s \times p_a$ stoichiometric matrix for the p_a chemisorption processes, $\boldsymbol{\xi}_a$ is a p_a dimensional vector containing the overall rates of chemisorption, \mathbf{N}_r^T is the $S_s \times R$ stoichiometric matrix for the R surface reactions, \mathbf{r} is a R dimensional vector of reaction rates on the catalyst surface. Note that the meaning of the matrix $\mathbf{E}_{m,g}$ is the same as in Equation 2.1 except that its dimension is $S_s \times p_m$.

For a solid phase containing S_s number of species, let us represent the set of ω adsorbed species on the catalyst sites as Ω , with $\omega = \dim(\Omega)$, the vacant active sites as $*$, and the set of ϕ non-adsorbed (free) gas species just above the solid surface as Φ , with $\phi = \dim(\Phi)$. Also, assume that the catalyst surface has only one type of active sites. Hence, the mole balance equations for all the S_s species of the solid phase can be divided in three components: $\mathbf{n}_{\Phi,s}$, the number of moles of the gas species just above the solid surface, $\mathbf{n}_{\Omega,s}$, the number of moles of the species adsorbed on the catalyst surface and $n_{*,s}$, the number of moles of vacant (free) active sites. Some properties of the matrices $\mathbf{E}_{m,s}$, \mathbf{N}_a^T and \mathbf{N}_r^T of Equation 2.3 can be seen if it is re-written as:

$$\begin{bmatrix} \dot{\mathbf{n}}_{s,\Phi}(t) \\ \dot{\mathbf{n}}_{s,\Omega}(t) \\ \dot{n}_{s,*}(t) \end{bmatrix} = \underbrace{\begin{bmatrix} \mathbf{E}_{m,s,\Phi} \\ \mathbf{0}_{\omega \times p_m} \\ \mathbf{0}_{1 \times p_m} \end{bmatrix}}_{\mathbf{E}_{m,s}} \boldsymbol{\xi}_m(t) + \mathbf{N}_a^T \boldsymbol{\xi}_a(t) + \underbrace{\begin{bmatrix} \mathbf{0}_{\phi \times R} \\ \mathbf{N}_{r,\Omega}^T \\ \mathbf{n}_{r,*}^T \end{bmatrix}}_{\mathbf{N}_r^T} \mathbf{r} \quad (2.4)$$

with $\mathbf{E}_{m,s,\Phi}$, $\mathbf{N}_{r,\Omega}^T$ and $\mathbf{n}_{r,*}^T$ of dimensions $\phi \times p_m$, $\omega \times R$ and $1 \times R$, respectively. Note that $S_s = \phi + \omega + 1$.

Note the particular structure of matrix $\mathbf{E}_{m,s}$. The particular structure of \mathbf{N}_r^T is only true if the set of species Φ are forced to adsorb before or desorb after being involved in any surface reaction. Importantly, the number of moles $\mathbf{n}_{\Omega,s}$ and $n_{*,s}$ are linearly dependent as stated in Section 1.4. Also, the p_a chemisorption processes and R surface reaction are assumed to be independent according to the definition proposed by Bhatt et al [9].

The total mass of all the species in the solid phase $m_s(t)$ can be calculated from the number of moles $\mathbf{n}_s(t)$ as

$$m_s(t) = \mathbf{1}_{S_s}^T \mathbf{M}_{w,s} \mathbf{n}_s(t), \quad m_s(0) = m_{0,s} \quad (2.5)$$

with $\mathbf{1}_{S_s}^T$ a S_s -dimensional vector of ones and $\mathbf{M}_{w,s}$ the S_s -dimensional diagonal matrix of molecular weights.

Chapter 3

Kinetic Identification using Extents

The concept of extents is discussed in this chapter in the context of Gas-Solid catalytic reaction systems. The concept of transformation of the number of moles in a chemical system is known for 60 years. Asbjørnsen and co-workers [11, 12, 13] introduced the concept of reaction variants and invariants and used it for the modelling of reactors. However, for open reactors, the reaction variants proposed in the literature are affected by the inlet and outlet flows and therefore represent more than the reaction contributions. Friedly [14, 15] proposed to compute the extents of *equivalent batch reactions*, associating the remainder to transport processes. This author then used them to describe the dynamics of flow through porous media accompanied by chemical reactions [16]. For open homogeneous reaction systems, Srinivasan et al. [17] developed a nonlinear transformation of the numbers of moles to reaction variants, flow variants, and reaction and flow invariants, thereby separating the effects of reactions and flows. Later, Amrhein et al. [2] refined that transformation to make it linear and therefore simpler. They also showed that, for a reactor with an outlet flow, the concept of vessel extent is most useful, as it represents the amount of material associated with a given process (reaction, transport) that is still in the vessel. Physically, extents can be understood as decoupled effects acting on a system. Bhatt et al. [18] extended that concept to heterogeneous Gas-Liquid reaction systems for the case of no reaction and no accumulation in the film, the result being decoupled vessel extents of reaction, mass transfer, inlet and outlet, as well as true invariants (i.e. identically equal to zero). Recently, Srinivasan et al. [19] further simplified the linear transformation and put a new glance on the concept of vessel extents.

This chapter explains the linear transformation of the number of moles in the gas and solid phases to corresponding vessel extents for a catalytic system. A method for computing the vessel extents as described in Srinivasan et al. [19] is adapted to calculate extents for this new type of system. These extents are then used to model the different kinetic processes of such a system.

3.1 Transformation to Extents

The transformation introduced by Bonvin and coworkers [18] for heterogeneous Gas-Liquid reaction systems is extended here to Gas-Solid catalytic reaction system, which are expressed as Equations 2.1 and 2.3. Two transformations are developed to express the number of moles in gas and solid phases (\mathbf{n}_g and \mathbf{n}_s , respectively) in terms of various (vessel) extents:

1. In the gas phase, \mathbf{n}_g is transformed to p_m extents of mass transfer, $\mathbf{x}_{m,g}$, p_g extents of inlets, $\mathbf{x}_{in,g}$, one extent of initial conditions, $x_{ic,g}$, and q_g extents of invariants, $\mathbf{x}_{iv,g}$.
2. In the solid phase, \mathbf{n}_s is transformed to R extents of reaction, \mathbf{x}_r , p_a extents of chemisorption (adsorption), \mathbf{x}_a , p_m extents of mass transfer, $\mathbf{x}_{m,s}$, and q_s extents of invariants, $\mathbf{x}_{iv,s}$.

3.1.1 Gas Phase

The gas phase follows the mole balance Equation 2.1. To obtain a meaningful transformation of the number of moles in the gas phase, \mathbf{n}_g is divided into four parts, namely p_g extents of inlet $\mathbf{x}_{in,g}$, p_m extents of mass transfer $\mathbf{x}_{m,g}$, one extent of initial conditions $x_{ic,g}$, and $q_g = S_g - (p_m + p_g + 1)$ extents of invariants $\mathbf{x}_{iv,g}$. These invariants are *true* invariant and complement the subspaces of the $p_m + p_g + 1$ variants up to the original S_g dimensional space.¹ They can be defined as a set of q_g linearly independent variables that evolve in a space orthogonal to the subspaces of mass transfer, inlet flow and initial conditions. Figure 3.1 represents the S_g dimensional space decomposed in the subspaces of inlets, mass transfers, initial condition and invariants.

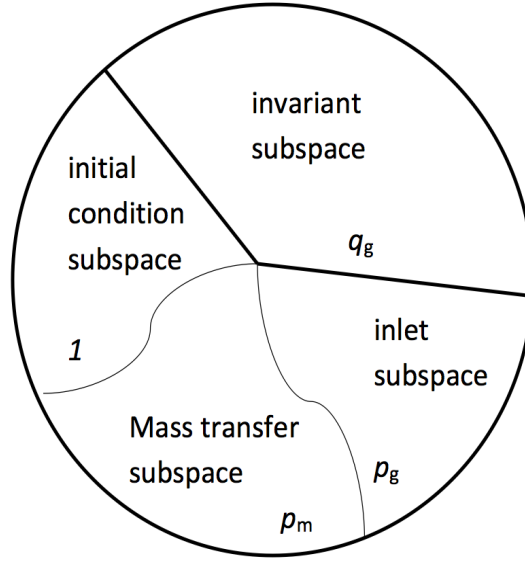


Figure 3.1: Decomposition of the S_g -dimensional space of the numbers of moles in the gas phase into a p_g -dimensional inlet subspace, a p_m -dimensional mass-transfer subspace, a one-dimensional subspace describing the contribution of the initial conditions and a q_g -dimensional invariant subspace.

The linear transformation \mathcal{T}_g that transforms the number of moles in the gas phase, \mathbf{n}_g , into extents is defined as

$$\begin{bmatrix} \mathbf{x}_{m,g}(t) \\ \mathbf{x}_{in,g}(t) \\ x_{ic,g}(t) \\ \mathbf{x}_{iv,g}(t) \end{bmatrix} = \mathcal{T}_g \mathbf{n}_g(t) = \begin{bmatrix} \mathbf{M}_g \\ \mathbf{F} \\ \mathbf{i}^T \\ \mathbf{Q}_g \end{bmatrix} \mathbf{n}_g(t) \quad (3.1)$$

The transformation brings Equation 2.1 to

¹In other words, linear transformation 3.1 implies $\underbrace{\mathbf{E}_{m,g} \mathbf{M}_g}_{\text{rank}(\cdot)=p_m} + \underbrace{\mathbf{W}_{in,g} \mathbf{F}}_{\text{rank}(\cdot)=p_g} + \underbrace{\mathbf{n}_{0,g} \mathbf{i}^T}_{\text{rank}(\cdot)=1} + \underbrace{\mathbf{P}_g \mathbf{Q}_g}_{\text{rank}(\cdot)=q_g} = \mathbf{I}_{S_g}$

$$\dot{\mathbf{x}}_{m,g}(t) = \boldsymbol{\xi}_m(t) - \frac{u_{out,g}(t)}{m_g(t)} \mathbf{x}_{m,g}(t), \quad \mathbf{x}_{m,g}(0) = \mathbf{0}_{p_m} \quad (3.2a)$$

$$\dot{\mathbf{x}}_{in,g}(t) = \mathbf{u}_{in,g}(t) - \frac{u_{out,g}(t)}{m_g(t)} \mathbf{x}_{in,g}(t), \quad \mathbf{x}_{in,g}(0) = \mathbf{0}_{p_g} \quad (3.2b)$$

$$\dot{x}_{ic,g}(t) = -\frac{u_{out,g}(t)}{m_g(t)} x_{ic,g}(t), \quad x_{ic,g}(0) = 1 \quad (\text{discounting } \mathbf{n}_{0,g}) \quad (3.2c)$$

$$\dot{\mathbf{x}}_{iv,g}(t) = -\frac{u_{out,g}(t)}{m_g(t)} \mathbf{x}_{iv,g}(t), \quad \mathbf{x}_{iv,g}(0) = \mathbf{0}_{q_g} \quad (3.2d)$$

where \mathbf{M}_g , \mathbf{F} , and \mathbf{Q}_g are matrices of dimensions $p_m \times S_g$, $p_g \times S_g$, and $q_g \times S_g$, respectively and \mathbf{i} is a vector of dimension S_g .

The transformation \mathcal{T}_g is constructed as

$$\mathcal{T}_g = [\mathbf{E}_{m,g} \quad \mathbf{W}_{in,g} \quad \mathbf{n}_{0,g} \quad \mathbf{P}_g]^{-1} \quad (3.3)$$

where \mathbf{P}_g is a $S_g \times q_g$ matrix representing the null space, such that $\mathbf{P}_g^T [\mathbf{E}_{m,g} \quad \mathbf{W}_{in,g} \quad \mathbf{n}_{0,g}] = \mathbf{0}_{q_g \times S_g - q_g}$ and hence it is orthogonal to all other subspaces. The transformation is such that

$$\begin{bmatrix} \mathbf{M}_g \\ \mathbf{F} \\ \mathbf{i}^T \\ \mathbf{Q}_g \end{bmatrix} [\mathbf{E}_{m,g} \quad \mathbf{W}_{in,g} \quad \mathbf{n}_{0,g} \quad \mathbf{P}_g] = \begin{bmatrix} \mathbf{I}_{p_m} & \mathbf{0} & \mathbf{0} & \mathbf{0} \\ \mathbf{0} & \mathbf{I}_{p_g} & \mathbf{0} & \mathbf{0} \\ \mathbf{0} & \mathbf{0} & 1 & \mathbf{0} \\ \mathbf{0} & \mathbf{0} & \mathbf{0} & \mathbf{I}_{q_g} \end{bmatrix}. \quad (3.4)$$

The number of moles can be reconstructed from the various extents by multiplying $\mathbf{n}_g(t)$ with \mathcal{T}_g and considering the fact that the extents of invariants $\mathbf{x}_{iv,g}(t)$ are equal to zero.

$$\mathbf{n}_g(t) = \mathbf{W}_{in,g} \mathbf{x}_{in,g}(t) - \mathbf{E}_{m,g} \mathbf{x}_{m,g}(t) + \mathbf{n}_{0,g} x_{ic,g}(t) \quad (3.5)$$

The gas phase with S_g species has formally S_g extents to be calculated, namely, $p_m + p_g + 1$ variant and q_g invariant states. If $\text{rank}([\mathbf{E}_{m,g} \quad \mathbf{W}_{in,g} \quad \mathbf{n}_{0,g}]) = p_m + p_g + 1$, the linear transformation \mathcal{T}_g brings Equation 2.1 to the system of Equations 3.2, as seen above. If $S_g < p_m + p_g + 1$, the transformation \mathcal{T}_g cannot be computed. This case is frequently encountered for the gas phase of Gas-Solid catalytic reaction systems. As all the species in the gas phase undergo mass transfer to the solid phase, $S_g = p_m$ and thus $S_g < p_m + p_g + 1$. In such a case, the extents in gas phase have to be computed via a Mass-transfer Variant (MV) form.

Let the matrices $\mathbf{E}_{m,g}$, $\mathbf{W}_{in,g}$ and the vector $\mathbf{n}_{0,g}$ be known. In addition, assume that $\mathbf{n}_g(t)$, $\mathbf{u}_{in}(t)$ and $u_{out}(t)$ are measured, $\text{rank}(\mathbf{E}_{m,g}) = p_m$ and $S_g = p_m$. Then, the p_m extents of mass transfer can be computed from the extents of inlet flow and initial conditions as follows,

$$\mathbf{x}_{in,g}(t) = \int_0^t \left(\mathbf{u}_{in,g}(\tau) - \frac{u_{out}(\tau)}{m_g(\tau)} \mathbf{x}_{out,g}(\tau) \right) d\tau, \quad \mathbf{x}_{out,g}(0) = \mathbf{0} \quad (3.6a)$$

$$x_{ic,g}(t) = -\int_0^t \frac{u_{out}(\tau)}{m_g(\tau)} x_{ic,g}(\tau) d\tau, \quad x_{ic,g}(0) = 1 \quad (3.6b)$$

$$\mathbf{x}_{m,g}(t) = -\mathbf{E}_{m,g}^{-1} \mathbf{n}_g^{MV}(t) = -\mathbf{E}_{m,g}^{-1} \left(\mathbf{n}_g(t) - \mathbf{W}_{in,g} \mathbf{x}_{in,g}(t) - \mathbf{n}_{0,g} x_{ic,g}(t) \right) \quad (3.6c)$$

Interpretation of the Transformation

Extents of Inlet Flow $\mathbf{x}_{in,g}$ [mass]: The element $x_{in,g,a}$, $\forall a \in \{1, \dots, p_g\}$, can be interpreted as the mass added by the a th inlet stream that remains in the reactor. The term $-\frac{u_{out,g}}{m_g} x_{in,g,a}$ accounts for the material added by the a th inlet that has left the reactor.

Extents of Mass Transfer $\mathbf{x}_{m,g}$ [moles]: The element $x_{m,g,b}$, $\forall b \in \{1, \dots, p_m\}$, corresponds to the mass transferred to the solid by the b th mass transfer and that is still in the reactor. As mentioned in Section 1.3, by convention, the mass transfer of a species that transfers from the gas to the solid phase is positive, whereas it is negative if it transfers from the solid to the gas phase. When positive, it can be interpreted as the number of moles of that species that would have accumulated and remained in the gas phase had there not been any mass transfer.

Extent of Initial Conditions $x_{ic,g}$ [-]: The scalar $x_{ic,g}$ indicates the fraction of the initial conditions that is still in the reactor. The value of $x_{ic,g}$ varies between 1 (initially) and 0 (all the initial numbers of moles have left the reactor).

Experimental Measurements

The numbers of moles in the gas phase can be measured over time by various types of spectrometry. Mid-infrared (MIR), near infrared (NIR) and ultraviolet/visible (UV/VIS) spectrometers measure indirectly the concentration of many species on-line during the course of a reaction, this with short sampling times and without disturbing the reaction [20]. Measurements of the number of moles in the gas phase can also be acquired by gas chromatography.

3.1.2 Solid Phase

The solid phase follows the mole balance Equation 2.3. To obtain a meaningful transformation of the number of moles in the solid phase, \mathbf{n}_s are divided into four parts, namely, p_m extents of mass transfer $\mathbf{x}_{m,s}$, p_a extents of chemisorption \mathbf{x}_a , R extents of reaction \mathbf{x}_r , and $q_s = S_s - (p_m + p_a + R)$ extents of invariants $\mathbf{x}_{iv,s}$. As there is no outlet term in the solid phase, the extent of initial conditions would constantly be equal to 1. Hence, one should consider the initial conditions as an invariant and remove their constant effect prior to applying the transformation into extents. The invariants complement the subspace of the $p_m + p_a + R$ variables up to the original S_s dimensional space.² They can be defined as a set of q_s linearly independent variables that evolve in the space orthogonal to the subspaces of mass transfer, chemisorption and reaction. Figure 3.2 represents the S_s dimensional space of the number of moles in the solid phase transformed into the subspaces of mass transfer, chemisorption, reactions and invariants.

The linear transformation \mathcal{T}_s transforms \mathbf{n}_s into

$$\begin{bmatrix} \mathbf{x}_{m,s}(t) \\ \mathbf{x}_a(t) \\ \mathbf{x}_r(t) \\ \mathbf{x}_{iv,s}(t) \end{bmatrix} = \mathcal{T}_s (\mathbf{n}_s(t) - \mathbf{n}_{0,s}) = \begin{bmatrix} \mathbf{M}_s \\ \mathbf{A} \\ \mathbf{R} \\ \mathbf{Q}_s \end{bmatrix} (\mathbf{n}_s(t) - \mathbf{n}_{0,s}) \quad (3.7)$$

This linear transformation brings Equation 2.3 to

$$\dot{\mathbf{x}}_{m,s}(t) = \boldsymbol{\xi}_m(t) \quad \mathbf{x}_{m,s}(0) = \mathbf{0}_{p_m} \quad (3.8a)$$

$$\dot{\mathbf{x}}_a(t) = \boldsymbol{\xi}_a(t) \quad \mathbf{x}_a(0) = \mathbf{0}_{p_a} \quad (3.8b)$$

$$\dot{\mathbf{x}}_r(t) = \mathbf{r}(t) \quad \mathbf{x}_r(0) = \mathbf{0}_R \quad (3.8c)$$

$$\dot{\mathbf{x}}_{iv}(t) = \mathbf{0}_{q_s} \quad \mathbf{x}_{iv}(0) = \mathbf{0}_{q_s} \quad (3.8d)$$

²In other words, linear transformation 3.7 implies $\underbrace{\mathbf{E}_{m,s} \mathbf{M}_s}_{\text{rank}(\cdot)=p_m} + \underbrace{\mathbf{N}_a^T \mathbf{A}}_{\text{rank}(\cdot)=p_a} + \underbrace{\mathbf{N}_r^T \mathbf{R}}_{\text{rank}(\cdot)=R} + \underbrace{\mathbf{P}_s \mathbf{Q}_s}_{\text{rank}(\cdot)=q_s} = \mathbf{I}_{S_s}$

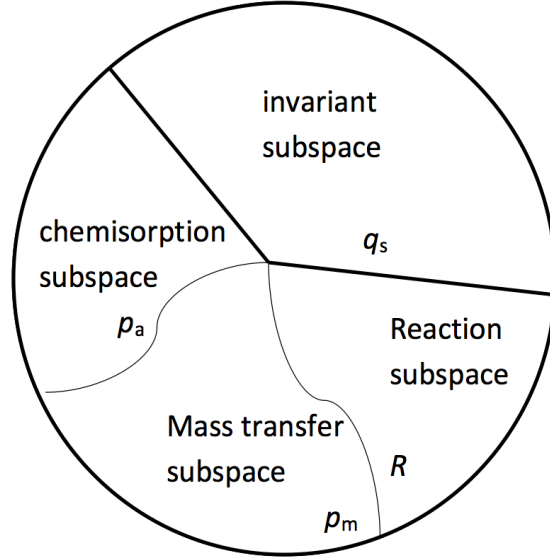


Figure 3.2: Decomposition of the S_s -dimensional space of the numbers of moles in the solid phase into a p_m -dimensional mass transfer subspace, a p_a -dimensional chemisorption subspace, a R -dimensional reaction subspace and a q_s -dimensional invariant subspace.

where \mathbf{M}_s , \mathbf{A} , \mathbf{R} and \mathbf{Q}_s are matrices of dimensions $p_m \times S_s$, $p_a \times S_s$, $R \times S_s$ and $q_s \times S_s$. Note that the extents of invariants $\mathbf{x}_{iv,s}$ are constantly equal to zero.

The transformation for the solid phase is constructed as

$$\mathcal{T}_s = [\mathbf{E}_{m,s} \quad \mathbf{N}_a^T \quad \mathbf{N}_r^T \quad \mathbf{P}_s]^{-1} \quad (3.9)$$

where \mathbf{P}_s is a $S_s \times q_s$ matrix representing the null space such that $\mathbf{P}_s^T [\mathbf{E}_{m,s} \quad \mathbf{N}_a^T \quad \mathbf{N}_r^T] = \mathbf{0}_{q_s \times (S_s - q_s)}$ and hence orthogonal to all other subspaces. The transformation is such that

$$\begin{bmatrix} \mathbf{M}_s \\ \mathbf{A} \\ \mathbf{R} \\ \mathbf{Q}_s \end{bmatrix} [\mathbf{E}_{m,s} \quad \mathbf{N}_a^T \quad \mathbf{N}_r^T \quad \mathbf{P}_s] = \begin{bmatrix} \mathbf{I}_{p_m} & \mathbf{0} & \mathbf{0} & \mathbf{0} \\ \mathbf{0} & \mathbf{I}_{p_a} & \mathbf{0} & \mathbf{0} \\ \mathbf{0} & \mathbf{0} & \mathbf{I}_R & \mathbf{0} \\ \mathbf{0} & \mathbf{0} & \mathbf{0} & \mathbf{I}_{q_s} \end{bmatrix}. \quad (3.10)$$

The number of moles can be reconstructed from the various extents by multiplying $\mathbf{n}_s(t)$ with \mathcal{T}_s and considering that the extents of invariants $\mathbf{x}_{iv,s}(t)$ are equal to zero.

$$\mathbf{n}_s(t) = \mathbf{E}_{m,s} \mathbf{x}_{m,s}(t) + \mathbf{N}_a^T \mathbf{x}_a(t) + \mathbf{N}_r^T \mathbf{x}_r(t) + \mathbf{n}_0 \quad (3.11)$$

The solid phase with S_s species has formally S_s extents to be calculated, namely, $p_m + p_a + R$ variant and q_s invariant states. If $\text{rank}([\mathbf{E}_{m,s} \quad \mathbf{N}_a^T \quad \mathbf{N}_r^T]) = p_m + p_a + R$, the linear transformation brings Equation 2.3 to the system of Equations 3.8. However, for this kind of systems, some solid species are generally linearly dependent on others, that is $\text{rank}([\mathbf{E}_{m,s} \quad \mathbf{N}_a^T \quad \mathbf{N}_r^T]) < p_m + p_a + R$, and the transformation matrix \mathcal{T}_s cannot be computed. In such a case, the extents in solid phase have to be computed via a Reaction Adsorption Variant (RAV) form.

Let the matrices $\mathbf{E}_{m,s}$, \mathbf{N}_a , \mathbf{N}_r and the vector $\mathbf{n}_{0,s}$ be known. In addition, assume that $S_s = p_m + p_a + R$. Then, the p_a extents of chemisorption and the R extents of reaction can be computed from the extents of mass transfer, as follows:

1. Computation of the extents of mass transfer in solid phase $\mathbf{x}_{m,s}$ from the extents in gas phase $\mathbf{x}_{m,g}$

$$\boldsymbol{\delta}_m(t) = - \int_0^t \frac{u_{out}(\tau)}{m_g(\tau)} \mathbf{x}_{m,g}(\tau) d\tau \quad \boldsymbol{\delta}_m(0) = \mathbf{0}_{p_m} \quad (3.12)$$

$$\mathbf{x}_{m,s}(t) = \mathbf{x}_{m,g}(t) - \boldsymbol{\delta}_m(t) \quad (3.13)$$

2. Computation of the extents of chemisorption \mathbf{x}_a and of reaction \mathbf{x}_r in the solid phase.

$$[\mathbf{N}_a^T \quad \mathbf{N}_r^T] \begin{bmatrix} \mathbf{x}_a(t) \\ \mathbf{x}_r(t) \end{bmatrix} = \mathbf{n}_s^{RAV}(t) = \mathbf{n}_s(t) - \mathbf{n}_{0,s} - \mathbf{E}_{m,s} \mathbf{x}_{m,s}(t) \quad (3.14a)$$

$$\text{and} \quad \begin{bmatrix} \mathbf{x}_a(t) \\ \mathbf{x}_r(t) \end{bmatrix} = [\mathbf{N}_a^T \quad \mathbf{N}_r^T]^+ \mathbf{n}_s^{RAV}(t) \quad (3.14b)$$

Note that this Reaction Adsorption Variant (RAV) form is invariant with respect to mass transfer but variant with respect to chemisorption (physical process defined by convention as adsorption steps) and surface reaction (chemical process).

Interpretation of the Transformation

Extents of Mass Transfer $\mathbf{x}_{m,s}$ [moles]: The element $x_{m,s,i}, \forall i \in \{1, \dots, p_m\}$ corresponds to the mass transferred to the solid surface by the i th mass transfer. Similarly to the extents of mass transfer in the gas phase, $x_{m,s,i}$ is positive if a species transfers from the gas to the solid and is negative if it transfers from the solid to the gas. When negative, it can be interpreted as the number of moles of that species that would have accumulated and remained in the solid phase had there not been any mass transfer.

Extents of Chemisorption \mathbf{x}_a [moles]: The element $x_{a,j}, \forall j = \{1, \dots, p_a\}$, indicates the number of moles that is adsorbed or desorbed by the j th chemisorption process. As mentioned in Section 1.4, by convention, the adsorption of a species on the solid surface is positive, whereas the desorption of a species is negative.

Extents of Reaction \mathbf{x}_r [moles]: The element $x_{a,k}, \forall k = \{1, \dots, R_r\}$ is the number of moles that is produced by the k th reaction on the surface of the solid.

Measurements and Measurement Reduction

Spectroscopy such as Diffuse-Reflectance FTIR Spectroscopy as described by Prairie et al. [21] is one way to compute the coverage $\boldsymbol{\theta}_\Omega(t)$ of all species Ω on the solid surface.

Catalyst characterisation such as the nature and number of active sites on the surface and the total surface area can be obtained by several spectroscopic or volumetric methods as described in [22]. BET model based experiments are widely used volumetric methods to obtain the total surface area and the number of active sites of a catalyst.

As described above, the calculation of the extents in the solid phase requires the measurement of $p_m + p_a + R$ species. However, as the p_m extents of mass transfer in the solid phase can be deduced from the extents of mass transfer in the gas phase (see Equations 3.12 and 3.13), this reduces the requirement of measured species to $p_a + R$. Further reduction in the number of measured species can be achieved using the various isotherms mentioned in Section 1.4. A simple model that describes the chemisorption phenomenon is the Langmuir-Hinshelwood (L-H) model which has been introduced in Section 1.4. Knowing the equilibrium constants ($K_{a,i}$) of all chemisorption steps ($\forall i = 1, \dots, p_a$), the L-H model allows calculating the coverage ($\theta_s, s \in \Omega$) of an adsorbed species s if the pressure (p_s) of that species above the surface is known. The L-H relation between pressure and coverage of a species s is given by:

$$\theta_s(t) = \frac{K_{a,s} p_s(t)}{1 + \sum_{i=1}^{p_a} K_{a,i} p_i(t)} \quad (3.15)$$

Hence, by using this correlation, a further reduction of the measurements requirement to only R is possible.

3.2 Kinetic Identification

Kinetic identification and estimation of corresponding rate parameters is performed by comparing the extents computed from the measured numbers of moles with their values predicted by a model, and adjusting the rate parameters. This comparison is done individually for each extent (i.e. indirectly for each rate) in order to find the rate expression that fits the best the data among a set of rate candidates.

For the i th reaction, let $\hat{\mathbf{x}}_{r,i}$ and $\mathbf{x}_{r,i}$ denote the H -dimensional vectors of computed (according to the linear transformations) and simulated (according to a postulated rate law involving the parameters $k_{r,i}$) extents of reaction at H time instants. The following parameter estimation problem can be formulated:

$$\begin{aligned} \min_{k_{r,i}} J_{r,i} &= (\hat{\mathbf{x}}_{r,i} - \mathbf{x}_{r,i}(k_{r,i}))^T \mathbf{W}_{r,i} (\hat{\mathbf{x}}_{r,i} - \mathbf{x}_{r,i}(k_{r,i})) \\ \text{s.t. } \dot{x}_{r,i}(t, k_{r,i}) &= r_i(\mathbf{n}_s(t), k_{r,i}), \quad x_{r,i}(0) = 0 \\ &\text{with } k_{r,i}^L < k_{r,i} < k_{r,i}^U, \quad \forall i = 1, \dots, R \end{aligned} \quad (3.16)$$

where $J_{r,i}$ is the cost function to be minimized, $\mathbf{W}_{r,i}$ is the $H \times H$ weighting matrix, r_i is the rate of the i th reaction, which is a postulated rate expression depending on the measured number of moles \mathbf{n}_s and on the rate constant $k_{r,i}$ (assuming one parameter per reaction), which is adjusted between the bounds $k_{r,i}^L$ and $k_{r,i}^U$.

Similarly a cost function can be designed to estimate the chemisorption (adsorption) rates. For the j th chemisorption process, let $\hat{\mathbf{x}}_{a,j}$ and $\mathbf{x}_{a,j}$ denote the H -dimensional vectors of computed (according to the linear transformations) and simulated (according to a postulated rate expression involving the parameter $k_{a,j}$) extents of chemisorption at H time instants. The following parameter estimation problem can be formulated:

$$\begin{aligned} \min_{k_{a,j}} J_{a,j} &= (\hat{\mathbf{x}}_{a,j} - \mathbf{x}_{a,j}(k_{a,j}))^T \mathbf{W}_{a,j} (\hat{\mathbf{x}}_{a,j} - \mathbf{x}_{a,j}(k_{a,j})) \\ \text{s.t. } \dot{x}_{a,j}(t, k_{a,j}) &= \xi_{a,j}(\mathbf{n}_s(t), k_{a,j}), \quad x_{a,j}(0) = 0 \\ &\text{with } k_{a,j}^L < k_{a,j} < k_{a,j}^U, \quad \forall j = 1, \dots, p_a \end{aligned} \quad (3.17)$$

where $J_{a,j}$ is the cost function to be minimized, $\mathbf{W}_{a,j}$ is the $H \times H$ weighting matrix, $\xi_{a,j}$ is the rate of the j th chemisorption step, which is a postulated rate expression depending on the measured number of moles \mathbf{n}_s and on the rate coefficient $k_{a,j}$ (assuming one parameter per chemisorption), which is adjusted between the bounds $k_{a,j}^L$ and $k_{a,j}^U$.

Equations 3.16 and 3.17 are used to estimate the parameters of each rate of reaction or each rate of adsorption. Each estimation problem is solved numerically using Newton-Gauss Levenberg-Marquardt algorithm in order to minimize $J_{r,i}$ or $J_{a,j}$.

The estimated values are expected to lie within a confidence interval (typically 68%, 95% or 99% confidence level) so as to estimate the true values of rate coefficients. Because of the measurement noise, however, error propagation affects the accuracy and precision of the estimated parameters, which can lead to bias or to very large confidence intervals, respectively.

Chapter 4

Case Study

The computation of extents for Gas-Solid catalytic systems and its use for incremental model identification are illustrated in this chapter. The synthesis of ammonia under isothermal conditions is considered over a high-surface-area iron catalyst.

The first section describes the reaction conditions which were used to generate the simulated measurements presented in the second section. The profiles of the computed extents of inlet, outlet and initial conditions in the gas phase as well as the profiles of the computed extents of chemisorption, reaction and mass transfer in the solid phase are described in third section. In the last section, the kinetic models for the chemisorption and reaction steps are identified incrementally.

4.1 Reaction System

The experimental conditions are adapted from Nielsen [23] for the synthesis of ammonia from N_2 and H_2 gases using iron catalyst. However, in this thesis, experimental conditions are replicated for a CSTR instead of a PFR to avoid the varying profiles of concentrations along the space coordinate of the reactor. Ammonia synthesis is simulated for a constant volume reactor with a total pressure of 25 atm and for a yield of 20% [24]. The experimental set-up is described in Table 4.1.

Table 4.1: Reactor characteristics (taken from [22])

| Variable | Value |
|----------------------|----------------------|
| Reactor volume | 5 cm ³ |
| H_2 to N_2 ratio | 3 : 1 |
| Temperature | 380 °C |
| Inlet flowrate | 3 ml s ⁻¹ |

Other relevant data needed to simulate the reaction system such as the catalyst characterization are shown in Table 4.2, according to references [3, 5, 6, 7, 25].

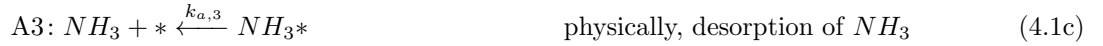
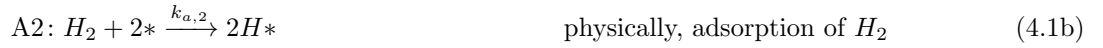
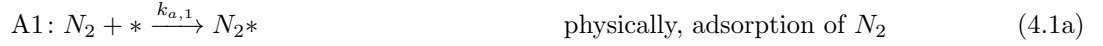
Table 4.2: Catalyst characteristics (taken from [3, 5, 6, 7, 24])

| Variable | Value |
|---|--|
| Weight of catalyst | 18 g |
| Specific surface area | 12 m ² g ⁻¹ |
| Total surface area (A) | 216 m ² |
| Total active sites | 6·10 ⁻² mol kg ⁻¹ |
| Total conc. of active sites (C_{tot}) | 5.1·10 ⁻⁶ mol m ⁻² |
| Diameter of pores | 1.5 mm |
| Radius of catalyst | 5 mm |
| Diffusion layer thickness (z) | 0.15 mm |
| Volume of catalyst | 2.5 cm ³ |

4.2 Simulated Measurements

Measurements for the gas and the solid phases are generated by numerical integration of Equation 2.1 and 2.3, respectively. This integration is done using MATLAB ODE stiff solver 'ode15s'. The initial amount of reactants H_2 and N_2 is 3 and 1 moles, respectively. The residence time in the reactor is maintained at 4.4 s, along with a constant ratio H_2 over N_2 of 3:1 in the inlet flowrate. The inlet and outlet mass flowrates are set constant at 11×10^{-3} kg s⁻¹ in order to maintain a constant volume. The mass-transfer rate ξ_m is obtained from the Equation 1.3 with diffusion coefficients $8.10 \cdot 10^{-4}$, $1.75 \cdot 10^{-4}$ and $9.75 \cdot 10^{-4}$ m²s⁻¹ for species N_2 , H_2 and NH_3 , respectively.

Species transferred to the solid are chemisorbed and react at the catalyst surface. Reactions at the solid surface take place in a set of cascade reactions following the Stoltze and Norskov model [24].



In Equations 4.1, symbols A followed by a number denote chemisorption steps (written by convention as adsorption steps) whereas symbols R followed by a number indicate reaction steps forming intermediates products. The Stoltze and Norskov model makes the assumption that there are no side reactions between the different nitrogen intermediates. According to the chemisorption/reaction scheme 4.1, the solid phase has 10 species whose number of moles are collected in the vector \mathbf{n}_s in the order $\{N_2, H_2, NH_3, N_2*, N*, H*, NH*, NH_2*, NH_3*, *\}$.

For this system, the matrices of inlet composition ($\mathbf{W}_{in,g}$), mass transfer in the gas phase and in the solid phase ($\mathbf{E}_{m,g}$ and $\mathbf{E}_{m,s}$), adsorption stoichiometry (\mathbf{N}_a) and reaction stoichiometry (\mathbf{N}_r) are as follows:

$$\mathbf{W}_{in,g} = \begin{bmatrix} 29.28 & 0 & 0 \\ 0 & 90 & 0 \\ 0 & 0 & 0 \end{bmatrix} \quad \mathbf{E}_{m,g} = \begin{bmatrix} 1 & 0 & 0 \\ 0 & 1 & 0 \\ 0 & 0 & 1 \end{bmatrix}$$

$$\mathbf{E}_{m,s} = \begin{bmatrix} 1 & 0 & 0 \\ 0 & 1 & 0 \\ 0 & 0 & 1 \\ 0 & 0 & 0 \\ 0 & 0 & 0 \\ 0 & 0 & 0 \\ 0 & 0 & 0 \\ 0 & 0 & 0 \\ 0 & 0 & 0 \\ 0 & 0 & 0 \end{bmatrix} \quad \mathbf{N}_a^T = \begin{bmatrix} -1 & 0 & 0 \\ 0 & -1 & 0 \\ 0 & 0 & -1 \\ 1 & 0 & 0 \\ 0 & 0 & 0 \\ 0 & 2 & 0 \\ 0 & 0 & 0 \\ 0 & 0 & 0 \\ 0 & 0 & 1 \\ 1 & -2 & -1 \end{bmatrix} \quad \mathbf{N}_r^T = \begin{bmatrix} 0 & 0 & 0 & 0 \\ 0 & 0 & 0 & 0 \\ 0 & 0 & 0 & 0 \\ -1 & 0 & 0 & 0 \\ 2 & -1 & 0 & 0 \\ 0 & -1 & -1 & -1 \\ 0 & 1 & -1 & 0 \\ 0 & 0 & 1 & -1 \\ 0 & 0 & 0 & 1 \\ -1 & 1 & 1 & 1 \end{bmatrix}$$

The rates of chemisorption and reactions are calculated using rate coefficients adapted from the Stoltze and Norskov model [24].¹

The number of moles adsorbed/desorbed by chemisorption ξ_a are calculated by the following rate expressions:

$$\xi_{a,1} = A k_{a,1} \mathcal{C}_{s,N_2} \mathcal{C}_{s,*}, \quad (4.2a)$$

$$\xi_{a,2} = A k_{a,2} \mathcal{C}_{s,H_2} \mathcal{C}_{s,*}^2, \quad (4.2b)$$

$$\xi_{a,3} = -A k_{a,3} \mathcal{C}_{s,NH_3*}, \quad (4.2c)$$

with $k_{a,1} = 1.48 \cdot 10^6 \text{ (mol/m}^2\text{)}^{-1}\text{s}^{-1}$, $k_{a,2} = 4.92 \cdot 10^{12} \text{ (mol/m}^2\text{)}^{-2}\text{s}^{-1}$ and $k_{a,3} = 6.10 \cdot 10^5 \text{ s}^{-1}$

The overall rates of reaction \mathbf{r} are calculated by the following rate expressions:

$$r_1 = A k_{r,1} \mathcal{C}_{s,N_2*} \mathcal{C}_{s,*}, \quad (4.3a)$$

$$r_2 = A k_{r,2} \mathcal{C}_{s,N*} \mathcal{C}_{s,H*}, \quad (4.3b)$$

$$r_3 = A k_{r,3} \mathcal{C}_{s,NH*} \mathcal{C}_{s,H*}, \quad (4.3c)$$

$$r_4 = A k_{r,4} \mathcal{C}_{s,NH_2*} \mathcal{C}_{s,H*}, \quad (4.3d)$$

with $k_{r,1} = 1.38 \cdot 10^9$, $k_{r,2} = 9.90 \cdot 10^{10}$, $k_{r,3} = 1.072 \cdot 10^9$ and $k_{r,4} = 8.00 \cdot 10^9$, all expressed in units $\text{(mol/m}^2\text{)}^{-1}\text{s}^{-1}$.

Table 4.3 summarizes the number of species and the number of dynamic effects involved in the catalytic synthesis of NH_3 .

Table 4.3: Number of species and number of dynamic effects involved in the synthesis of ammonia

| Phase | S_f | p_g | Outlet | p_m | p_a | R |
|-------|--------------|-------|--------|-------|-------|-----|
| Gas | 3 | 1 | 1 | 3 | 0 | 0 |
| Solid | 10^\dagger | 0 | 0 | 3 | 3 | 4 |

$$^\dagger S_s = \phi + \omega + 1 = 3 + 6 + 1 = 10$$

¹Adaptations are the following: as forward rate coefficients have higher orders of magnitude ($\gg 10^4$) than those of backward reactions, all reactions are approximated as forward steps only; values of forward rate coefficients are reduced to compensate the effect of backward reactions.

The initial number of moles in the solid and gas phase are assumed to be at the equilibrium, at values $\mathbf{n}_{s,0} = [N_2: 0.4, H_2: 1.2, NH_3: 0.03, N_2^*: 4.2 \times 10^{-4}, N^*: 2.4 \times 10^{-6}, H^*: 3.7 \times 10^{-4}, NH^*: 2 \times 10^{-4}, NH_2^*: 2.6 \times 10^{-5}, NH_3^*: 5.8 \times 10^{-7}, *: 6.58 \times 10^{-5}]$ moles for the solid phase and $\mathbf{n}_{g,0} = [N_2: 0.570, H_2: 1.71, NH_3: 0.04]$ moles for the gas phase.

The measurements are simulated from 0 to 8 seconds every 0.01 second during the first two seconds and then every 0.1 second until the steady state is reached (at 8 seconds). The simulated numbers of moles for the gas and the solid phase are corrupted with additive zero-mean Gaussian noise of standard deviation 1% with respect to the maximum concentration of each species. This leads to simulated measurements that will be referred to as the measurements in the rest of this thesis. Figure 4.1 shows these measurements for both phases.

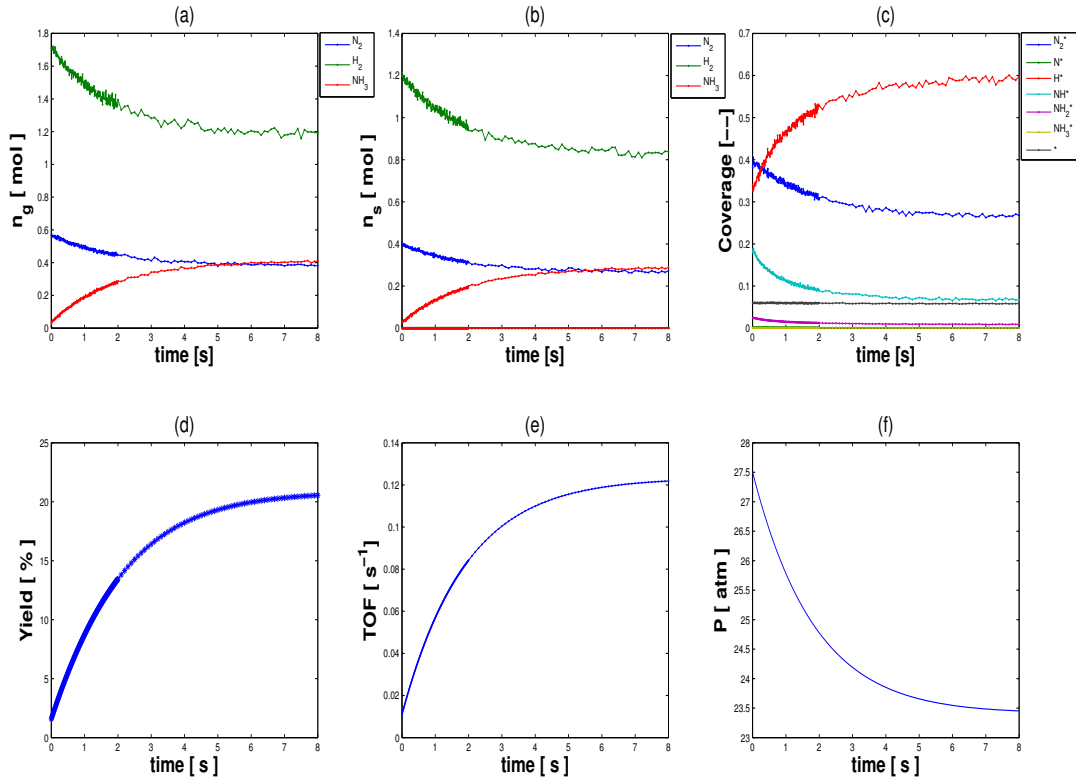


Figure 4.1: (Simulated) measurements of the number of moles in the gas phase (a) and in the solid phase (b), coverage of the reaction intermediates (c), reaction yield (d), turnover frequency (TOF) (e) and total pressure in the reactor (f) as a function of time.

As shown in Figure 4.1, the steady state is obtained a few seconds after the start of the reaction, which indicates that the catalytic reaction is very fast (see the magnitude of the rate coefficients in Equations 4.2 and 4.3). Figure 4.1a shows the change in the number of moles of the gas phase over time. The amount of reactants, N_2 and H_2 , initially decreases as these species are transferred to the solid phase and react. Eventually they reach a steady state. The number of moles of product, NH_3 , increases simultaneously in the gas phase as it is formed in the solid phase. Figure 4.1b represents the number of moles in the solid phase as a function of time. The species just above the solid surface $\Phi = \{N_2, H_2, NH_3\}$ follow the same profile as the corresponding species in the gas phase, but are of lesser magnitude.

The difference in magnitude is due to the resistance of mass transfer. The reaction intermediates $\Omega = \{N_2^*, N^*, H^*, NH^*, NH_2^*, NH_3^*\}$ and the vacant active sites (*), expressed in numbers of moles, are almost negligible at the solid surface. However, expressed in terms of coverage, they become visible (see Figure 4.1c) and their behavior is in agreement with the literature, both in terms of profile and magnitude. Figure 4.1d shows that the yield reaches 20 % at the steady state. For this reaction system, a turnover frequency (TOF)² of 0.12 s⁻¹ per active site is achieved (see Figure 4.1e) for a pressure of ca 25 atm (see Figure 4.1f)

4.3 Computation of Extents

Since $\text{rank}(\mathbf{E}_{m,g}) = p_m = 3$ and $\text{rank}([\mathbf{N}_a^T \ \mathbf{N}_r^T]) = p_a + R = 3 + 4 = 7$ (see Chapter 3 for the derivation of these rank conditions), the number of moles in each phase can be transformed to extents, as shown in Figure 4.3. Figure 4.3 shows that the extent of inlet is zero initially and increases until it reaches a steady state after 8 seconds. The extent of initial conditions varies between 1 and 0, zero being almost reached at the steady state, which indicates that there is almost nothing left from the initial conditions. The extent of mass transfer is positive for species N_2 and H_2 , that is, these species transfer from the gas to the solid phase, and is negative for species NH_3 , which on the contrary transfers from the solid to the gas phase. Note that the extents of mass transfer reach a steady state, however earlier than the extent of inlet or the extent of initial conditions.

In the solid phase, the extents of mass transfer for species N_2 and H_2 which transfer from the gas to the solid phase are positive and the extent of mass transfer for NH_3 is negative as it transfers from the solid to the gas phase. Figure 4.3e shows the $p_a = 3$ extents of chemisorption for the three gas species that are just in contact with the surface of the solid. The two adsorbed species N_2 and H_2 have a positive extent of chemisorption, which indicates that they adsorb on the solid surface, whereas the extent of chemisorption for the species NH_3 is negative, which implies that it is desorbed from the surface. The adsorption of N_2 is the slowest chemisorption process amongst all three. Figure 4.3f shows the extents of the $R = 4$ reactions at the solid surface over time. The extent of the first reaction (R1) is the smallest among all the four reactions, which indicates that reaction R1 (the dissociation of the adsorbed molecule of nitrogen N_2^* in adsorbed atoms of nitrogen N^*) is limiting the production of ammonia. More importantly, the extent of the first reaction (R1) equals the first extent of chemisorption (A1), which represents the adsorption of N_2 . This clearly indicates that the reaction step R1 is limited by the adsorption step A1. Therefore, the rate determining step among all chemisorption (A1-A3) and reaction (R1-R4) processes taking place in the ammonia synthesis can clearly be identified as the molecular adsorption of N_2 .

The next step consists in identifying the reaction and chemisorption rate expressions and estimating their rate coefficients in order to assess quantitatively the differences in the rates of chemisorption compared to surface reactions.

²The turnover frequency (TOF) is defined as the maximum number of molecules of substrate that a catalyst can convert to product per catalytic site and per unit of time.

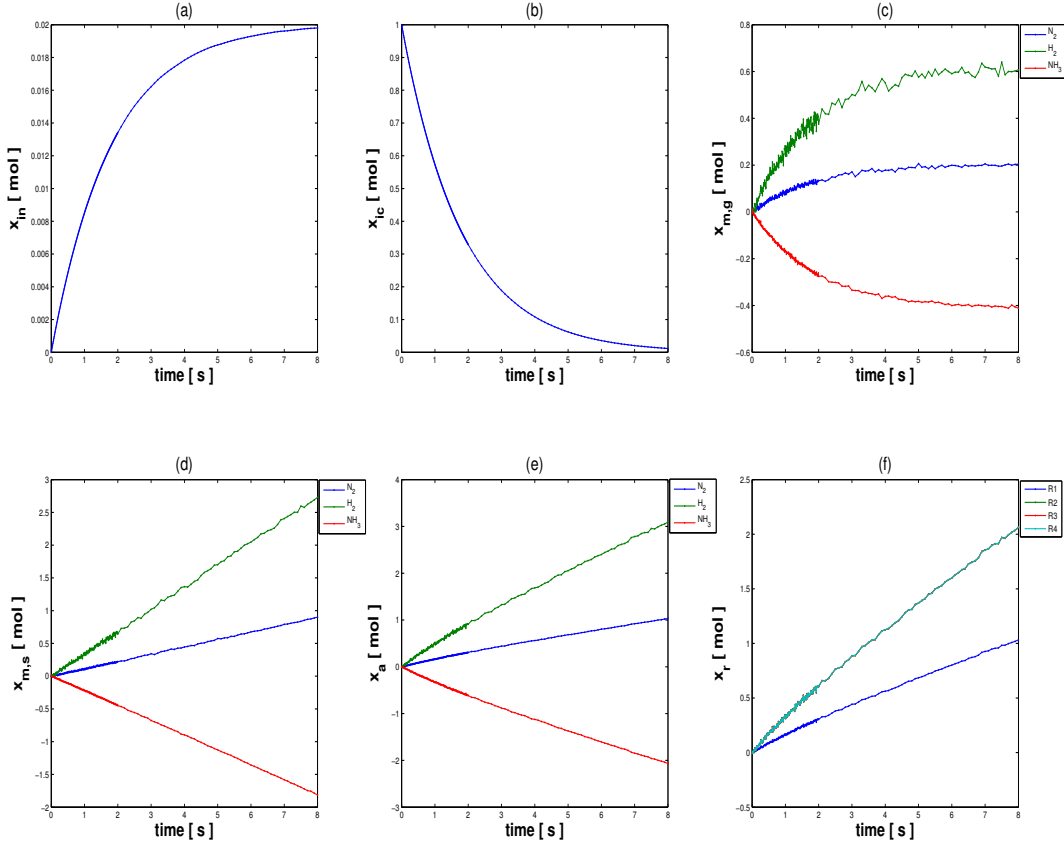


Figure 4.2: Extents of inlet ($\mathbf{x}_{in,g}$, diagram A), of initial conditions ($\mathbf{x}_{ic,g}$, diagram B) and of mass transfer ($\mathbf{x}_{m,g}$, diagram C) in the gas phase and extents of mass transfer ($\mathbf{x}_{m,s}$, diagram D), of chemisorption (\mathbf{x}_a , diagram E) and of reaction (\mathbf{x}_r , diagram F) in the solid phase as a function of time.

4.4 Identification of Rate Expressions

For each reaction, a candidate rate expression is integrated and fitted to the corresponding computed extent using the estimation problem formulated in section 3.2. For all chemisorption and reaction steps, the rate coefficients and their 99% confidence intervals corresponding to the identified rate expressions are compared with their true values in Table 4.5 and Table 4.4, respectively. Since the noise level is not too high, the identified rate expressions correspond to the rate expressions used for the simulation of the data. The extents computed from the measurements and those obtained by integration of the identified rate expressions are very close to each other as shown in Figure 4.3. Since chemisorption and surface reaction are extremely fast dynamic processes, small deviations from the true curves can be explained by round-off error and by the machine precision.

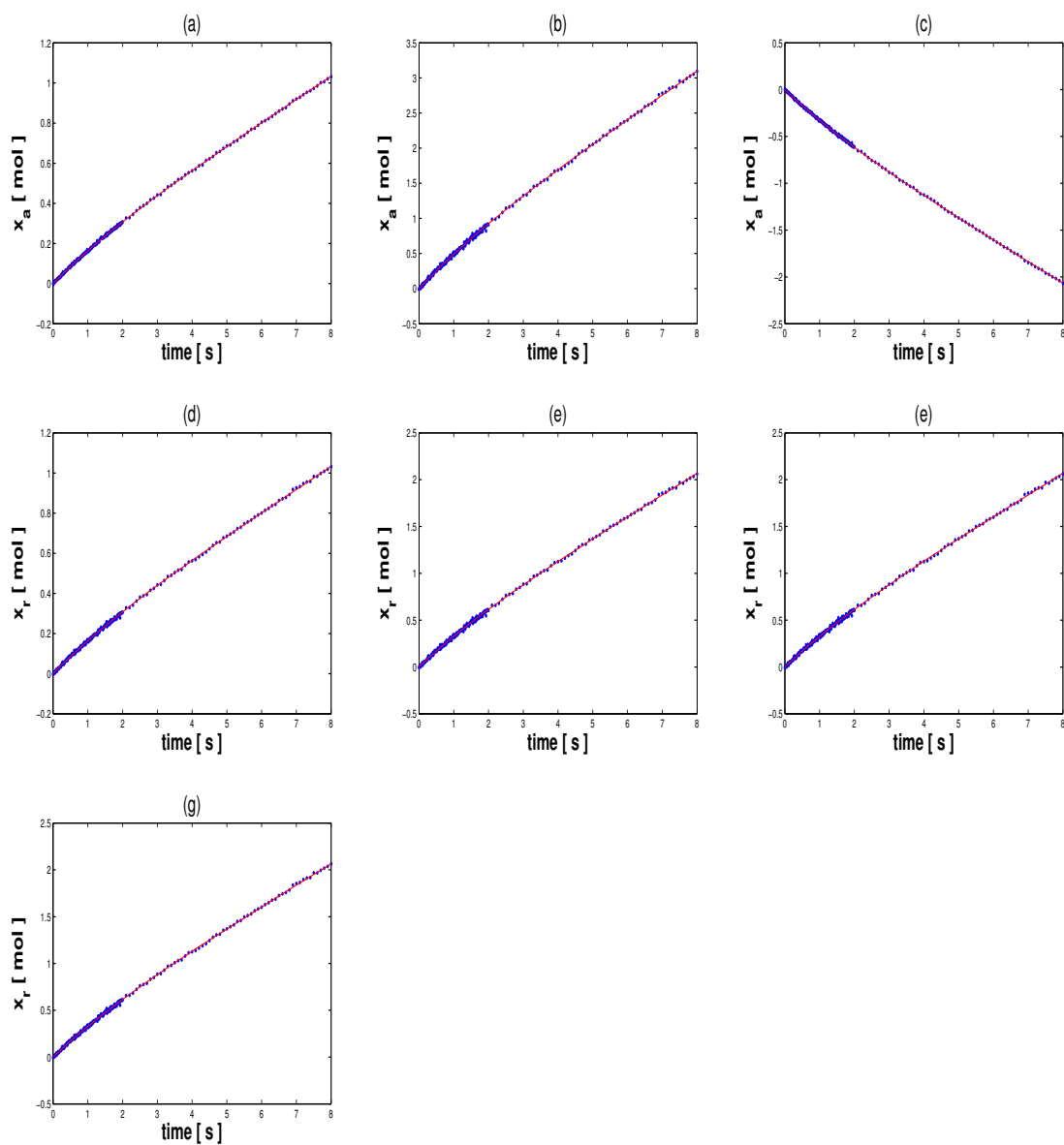


Figure 4.3: Extents of chemisorption (A: $x_{a,1}$, B: $x_{a,2}$ and C: $x_{a,3}$) and of reaction (D: $x_{r,1}$, E: $x_{r,2}$, F: $x_{r,3}$ and G: $x_{r,4}$) over time obtained by transformation of the measured numbers of moles (in blue) and integration of the correctly identified rate expression (in red).

Table 4.4: Identified rate expressions and estimated rate constants in $(\text{mol}/\text{m}^2)^{-1}\text{s}^{-1}$ (with 99% confidence intervals, C.I.) for all reaction steps of the synthesis of ammonia.

| Step | Identified model | Parameter | True | Estimated | C.I.(99%) |
|------|------------------|-----------|-----------------------|-----------------------|--------------------------------|
| R1 | Eq. 4.3a | $k_{r,1}$ | $1.380 \cdot 10^9$ | $1.379 \cdot 10^9$ | $[1.376, 1.382] \cdot 10^9$ |
| R2 | Eq. 4.3b | $k_{r,2}$ | $9.900 \cdot 10^{10}$ | $9.893 \cdot 10^{10}$ | $[9.864, 9.922] \cdot 10^{10}$ |
| R3 | Eq. 4.3c | $k_{r,3}$ | $1.072 \cdot 10^9$ | $1.072 \cdot 10^9$ | $[1.069, 1.074] \cdot 10^9$ |
| R4 | Eq. 4.3d | $k_{r,4}$ | $8.000 \cdot 10^9$ | $8.011 \cdot 10^9$ | $[7.991, 8.031] \cdot 10^9$ |

Table 4.5: Identified rate expressions and estimated rate coefficients (with 99% confidence intervals, C.I.) for all chemisorption steps involved in the synthesis of ammonia.

| Step | Identified model | Parameter | True | Estimated | C.I.(99%) |
|------|------------------|-------------|-----------------------|-----------------------|--------------------------------|
| A1 | Eq. 4.2a | $k_{a,1}^a$ | $1.480 \cdot 10^6$ | $1.480 \cdot 10^6$ | $[1.478, 1.483] \cdot 10^6$ |
| A2 | Eq. 4.2b | $k_{a,2}^b$ | $4.922 \cdot 10^{12}$ | $4.922 \cdot 10^{12}$ | $[4.908, 4.936] \cdot 10^{12}$ |
| A3 | Eq. 4.2c | $k_{a,3}^c$ | $6.100 \cdot 10^5$ | $6.100 \cdot 10^5$ | $[6.090, 6.109] \cdot 10^5$ |

^a in $(\text{mol}/\text{m}^2)^{-1}\text{s}^{-1}$

^b in $(\text{mol}/\text{m}^2)^{-2}\text{s}^{-1}$

^c in s^{-1}

Chapter 5

Conclusion

Catalytic reaction systems depend on a combination of several dynamic effects, such as the mass transfers, the chemisorption steps and the surface reactions occurring simultaneously. The rate coefficients of all these phenomena vary with the experimental conditions (e.g. temperature, stirring speed). As all these effects are interdependent, a slight change in any of these experimental conditions can change the overall dynamics of the system. Thus, to study the effect of each individual dynamic effect on the overall kinetics, it is of great advantage if one can decouple these processes. A methodology called ‘Extent-based Model Identification’ was used here to separate the effects taking place in heterogeneous gas-solid reaction systems, namely mass transfers, chemisorption steps, surface reactions, initial conditions, and inlet and outlet flows, in the form of (vessel) extents, which represent the contributions of each individual dynamic effect. Following this transformation step to extents, one can perform the task of model identification and parameter estimation based on each extents, that is, based on each individual dynamic effect.

As reactions involved in heterogeneous catalytic systems are very fast (the steady state is attained within a few seconds), obtaining extents for such systems requires a large amount of concentration measurements at the start of the reaction. Under this condition, the measured number of moles in the gas phase can be transformed into extents of mass transfer, inlet and outlet flows and the number of moles in the solid phase into extents of mass transfer, chemisorption and reaction. Information regarding the stoichiometry, the inlet composition, the transferring species and the initial conditions are required to compute these extents. Because most gas-phase species involved in catalytic reaction systems undergo mass transfer to the solid phase, the transformation of gas-phase measurements to extents has generally to be made via a Mass-transfer Variant (MV) form. In addition, as several chemisorption and surface reaction steps take place at the surface of the solid, solid-phase measurements have generally to be transformed to extents using a Reaction Adsorption Variant (RAV) form comprising the chemisorption and reactions steps. Furthermore, in case of large number of chemisorption or surface reaction steps, it may be required to apply further simplifications in the solid phase such as steady-state chemisorption which allows modelling the system with isotherms, such as the Lingmuir-Hinshelwood (L-H) model.

The proposed methodology has been validated using the case study of ammonia synthesis over an iron catalyst. Model identification of that system led to the following conclusions. First, as previously mentioned, catalytic reactions, and in particular the synthesis of ammonia, are very fast systems and hence, the extent-based model identification method requires a sufficiently large amount of concentration measurements at the start of the reaction. Second, the modelling of such systems is subjected to round-off errors and are sometimes even limited by the machine precision. Third, kinetic identification is difficult for dynamic systems involving rate processes (and rate coefficients) differing by several orders of magnitude ($\gg 10^4$ in the case of the ammonia synthesis). In particular, for reversible surface reactions or chemisorption reactions, with much lower backward than forward rate constants, the forward reaction direction was only considered. Once remedies have been taken to compensate for these limitations (high sampling time, right experimental conditions and use of forward reactions only), it was possible to model the kinetics of this catalytic system, that is, to correctly identify the rate models for the chemisorption steps and the surface reactions and to

reliably estimate their rate parameters within 99% confidence intervals.

Future work should concentrate on the application of the proposed methodology to more complex catalytic schemes where the number of intermediate species is higher. In this situation, the use of isotherm steady-state equations such as the L-H model would be required.

Bibliography

- [1] A. E. Croce, "The application of the concept of extent of reaction", *J. Chem. Educ.*, 79(4):506, 2002.
- [2] M. Amrhein et al., "Extents of Reaction and Flow for Homogeneous Reaction Systems with Inlet and Outlet Streams", *AIChE J.*, 56:2873, 2010.
- [3] H. S. Fogler, "Chemical Reaction Engineering", Prentice Hall, 4th Ed., 2005.
- [4] T. K. Sherwood and C. R. Wilke, "Mass Transfer", McGraw-Hill Kogakushu, New York, 1975.
- [5] R. Taylor and R. Krishna, "Multicomponent Mass Transfer", John Wiley & Sons, 1st Ed., New York, 1993.
- [6] R. Krishna, J. Wesselingh, "The Maxwell-Stefan approach to mass transfer", *Chem. Eng. Sci.*, 52(6):861, 1997.
- [7] E. A. Mason and A. P. Malinauskas, "Gas Transport in Porous Media: The Dusty Gas Model", Elsevier, Amsterdam, The Netherlands, 1983.
- [8] K. Y. Foo, B. H. Hameed, "Insights into the modeling of adsorption isotherm systems", *Chem. Eng. J.*, 156:2, 2010.
- [9] K. Christmann, "Thermodynamics and Kinetics of Adsorption", IMPRS-Lecture Series 2012: Experimental and Theoretical Methods in Surface Science, Institut für Chemie und Biochemie, Freie Universität Berlin, 2012.
- [10] N. Bhatt et al., "Extents of Reaction, Mass Transfer and Flow for Gas-Liquid Reaction Systems", *Ind. Eng. Chem. Res.*, 49:7704, 2010.
- [11] O. A. Asbjørnsen, M. Fjeld, "Response modes of continuous stirred tank reactors", *Chem. Eng. Sci.*, 25:1627, 1970.
- [12] O. A. Asbjørnsen, "Reaction invariants in the control of continuous chemical reactors", *Chem. Eng. Sci.*, 27:709, 1972.
- [13] M. Fjeld et al., "Reaction invariants and their importance in the analysis of eigenvectors, state observability and controllability of the continuous stirred tank reactor", *Chem. Eng. Sci.*, 29:1917, 1974.
- [14] J. C. Friedly, "Extent of reaction in open systems with multiple heterogeneous reactions", *AIChE J.*, 37(5):687, 1991.
- [15] J. C. Friedly, "Reaction coordinates for heterogeneous flow reactors: Physical interpretation", *AIChE J.*, 42(10):2987, 1996.
- [16] J. C. Friedly and J. Rubin, "Solute transport with multiple equilibrium-controlled or kinetically controlled chemical reactions", *Water Resources Research*, 28(6):1935, 1992.
- [17] B. Srinivasan et al., "Reaction and flow variants/invariants in chemical reaction systems with inlet and outlet streams", *AIChE J.*, 44(8):1858, 1998.

- [18] N. Bhatt et al., "Extents of reaction, mass transfer and flow for gas-liquid reaction systems", *Ind. Eng. Chem. Res.*, 49:7704, 2010.
- [19] S. Srinivasan et al., "Variant and Invariant States for Reaction Systems", *1st IFAC Workshop on Thermodynamic Foundations of Mathematical Systems Theory*, Lyon, 2013.
- [20] N. Bhatt, "Extents of Reaction and Mass Transfer in the Analysis of Chemical Reaction Systems", Doctoral Thesis n° 5028, EPF Lausanne, 2011.
- [21] M. Prairie et al., "Diffuse-Reflectance FTIR Spectroscopy for kinetic and Mechanistic studies of CO₂ hydrogenation in a Continuous recycle reactor", *Chem. Eng. Sci.*, 46:113, 1991.
- [22] G. Bergeret and P. Gallezot, "Particle Size and Dispersion Measurements, Handbook of Heterogeneous Catalysis", Wiley-VCH, 2008.
- [23] A. Nielson, "An Investigation of Promoted Iron Catalyst for Synthesis of Ammonia", Gjellerup, Copenhagen, 1968.
- [24] J. Dumesic and A. Trevino "Kinetic Simulation of Ammonia Synthesis Catalysis", *J. Catal.*, 116:119, 1989.
- [25] Gudmund Smedler, "Elementary Modelling Of Hydrogenation Kinetics on The Working Catalyst Surface", Doctoral Thesis, Department of Chemical Reaction Engineering, Chalmers University of Technology Göteborg, Sweden, 1987.